International Journal of Applied Mathematics
Volume 38 No. 8s, 2025
ISSN: 1311-1728 (printed version); ISSN: 1314-8060 (on-line version)

ECO-FRIENDLY FABRICATION AND ELECTROCHEMICAL EVALUATION OF Mn_2O_3, CuO, AND Mn_2O_3/CuO NANOCOMPOSITE FOR ENERGY STORAGE APPLICATIONS

Vangapandu Anusha[1], Budithi Ravi Kumar[2]*.

[1,2]Department of Physics, Andhra University, Visakhapatnam, Andhra Pradesh 530003, India.

*Corresponding Author: Dr. Budithi Ravi Kumar
*Email: ravi_budithi@yahoo.com

Abstract

The synthesis of manganese oxide (Mn_2O_3), copper oxide (CuO), and their composite (Mn_2O_3/CuO) nanoparticles was successfully achieved through an eco-friendly, cost-effective, and rapid green synthesis approach. This study investigates the influence of particle size on the electrochemical behavior of Mn_2O_3, CuO, and Mn_2O_3/CuO nanoparticle electrodes for supercapacitor applications. The surface morphology of the prepared materials was examined using field emission scanning electron microscopy (FESEM), while Fourier-transform infrared (FTIR) spectroscopy confirmed the presence of key functional groups. Electrochemical performance was evaluated through cyclic voltammetry (CV), electrochemical impedance spectroscopy (EIS) analysis. The CV curves of all electrodes exhibited pseudocapacitive behavior, with the Mn_2O_3/CuO composite displaying the highest specific capacitance. The specific capacitance (Cs) values at a scan rate of 10 mV s^{-1} were 73.66 F g^{-1} for Mn_2O_3, 148.72 F g^{-1} for CuO, and 249.39 F g^{-1} for Mn_2O_3/CuO, decreasing with increasing scan rate due to limited ion diffusion. Furthermore, EIS analysis revealed that the Mn_2O_3/CuO composite possessed lower charge-transfer resistance and improved ion diffusion, confirming its enhanced electrochemical kinetics and superior performance as a promising electrode material for high-performance supercapacitors.

Keywords: Green synthesis, Manganese Oxide (Mn_2O_3), Copper Oxide (CuO) and Mn_2O_3/CuO nanomaterials, supercapacitor, cyclic voltammeter (CV), electrochemical impedance spectroscopy (EIS) , electrochemical studies.

1.Introduction

The rapid advancement of nanotechnology has created new opportunities for designing multifunctional nanomaterials with tunable properties for energy storage applications [1,2]. Among various candidates, transition metal oxides such as manganese oxide (Mn_2O_3) and copper oxide (CuO) have gained considerable attention due to their distinctive physicochemical properties, low cost, and environmental compatibility [3]. Their excellent electrochemical activity, structural versatility, and semiconducting behavior make them promising materials for supercapacitor applications [4,5]. The synthesis of Mn_2O_3/CuO nanocomposites aims to combine the advantages of both oxides, resulting in synergistic effects that enhance charge separation, electrical conductivity, and electrochemical stability [6,7]. Supercapacitors, recognized as next-generation energy storage devices, are valued for their high-power density, fast charge–discharge capability, and long cycle life [8]. Transition metal oxides, particularly Mn_2O_3 and CuO, have been extensively investigated for their pseudocapacitive behavior [9]. Mn_2O_3 offers multiple oxidation states and environmental benignity, while CuO provides high theoretical capacitance and superior electrical conductivity [10]. Furthermore, the formation of

Received: August 10, 2025

International Journal of Applied Mathematics
Volume 38 No. 8s, 2025
ISSN: 1311-1728 (printed version); ISSN: 1314-8060 (on-line version)

a Mn_2O_3/CuO heterojunction can significantly improve charge transport and broaden the electrochemical potential window, which is essential for high-performance supercapacitors [11]. Depending on the synthesis route and composition, Mn_2O_3/CuO nanocomposites may also display interesting magnetic properties [12]. Various synthesis methods—including hydrothermal, co-precipitation, electrospinning, sol–gel, and chemical vapor deposition—have been reported for fabricating Mn_2O_3/CuO composites [1,2,13,14,15]. Current research focuses on understanding structure–property correlations, optimizing synthesis processes, and exploring multifunctional applications in energy storage, biomedicine, and environmental remediation [7,16]. However, pure Mn_2O_3 and CuO suffer from low-rate capability and limited cyclic stability, which can be effectively mitigated through composite formation strategies involving multiple metal oxides [5,17].

In this work, pure Mn_2O_3, CuO, and Mn_2O_3/CuO nanocomposites were synthesized, characterized, and comparatively analyzed to evaluate their structural and electrochemical properties. Emphasis was placed on investigating their charge storage performance to assess their potential for high-performance supercapacitor applications.

2. Experimental

2.1 Synthesis of Materials

2.2.1 Green synthesis of Mn_2O_3 nanoparticles

Mn_2O_3 nanoparticles were synthesized by mixing 25 mL of *Ocimum tenuiflorum* leaf extract with 50 mL of 5 mM $Mn(NO_3)_2{\cdot}4H_2O$, adjusting the pH to 9 with 6 M NaOH, and stirring for 24 hours. The product was filtered, dried at 120°C for 3 hours, calcined at 400°C for 2 hours, and stored in a sealed container for later use.

2.1.2 Green Methods of CuO Nanoparticles

CuO nanoparticles were synthesized by mixing 25 mL of *Ocimum tenuiflorum* leaf extract with 50 mL of 5 mM $Cu(NO_3)_2{\cdot}4H_2O$, adjusting the pH to 9 with 6 M NaOH, and stirring for 24 hours at room temperature. The product was filtered (0.22 μm), dried at 120°C for 3 hours, and calcined at 400°C for 2 hours to obtain CuO nanoparticles, which were stored in a sealed container for further use.

2.2.3 Green synthesis of Mn_2O_3/CuO nanocomposite

Mn_2O_3/CuO nanocomposite was synthesized via a one-pot method by mixing 40 mL of *Ocimum tenuiflorum* extract with 150 mL of deionized water, adding 1 g each of $Mn(NO_3)_2{\cdot}4H_2O$ and $Cu(NO_3)_2{\cdot}4H_2O$, and stirring at 45°C for 2 h. The pH was adjusted to 10 with NH_4OH, then the mixture was left for 12 h, filtered, and dried at 35°C for 24 h to obtain the *Ocimum tenuiflorum*–derived Mn_2O_3/CuO nanocomposite.

2.2 Characterization Techniques

The surface morphology was examined using a field emission scanning electron microscope (FE-SEM, Carl Zeiss, Ultra Plus) with samples mounted on carbon tape. Functional groups were identified through FTIR analysis (FTIR-4200). Electrochemical studies were performed at room temperature using a Metrohm Autolab PGSTAT302N potentiostat/galvanostat controlled by Nova 2.0.2 software (ECO Chemie, Netherlands) with a three-electrode screen-printed electrode (SPE, Dropsens, Spain). All reagents used were of analytical grade.

2.3 Electrochemical Measurements

Mn_2O_3/CuO nanoparticles were mixed with carbon black and PVDF (polyvinylidene fluoride) binder in a weight ratio of 8:1:1 to fabricate the working electrode. NMP (N-methyl-2-

Received: August 10, 2025

International Journal of Applied Mathematics
Volume 38 No. 8s, 2025
ISSN: 1311-1728 (printed version); ISSN: 1314-8060 (on-line version)

pyrrolidone) was used as a solvent, and the mixture was thoroughly ground using an agate mortar and pestle to obtain a homogeneous slurry. The resulting slurry was drop-cast onto Ni foam and dried at 100 °C. Electrochemical measurements were performed using a three-electrode setup, with the NiO nanoparticle electrode as the working electrode, platinum wire as the counter electrode, and Ag/AgCl as the reference electrode in 2 M KOH electrolyte. The electrochemical properties were analyzed using an OrigaLys 500 workstation through cyclic voltammetry (CV) within a potential window of 0.1–0.5 V.

3. Result and Discussion:

3.1 Morphological Analysis

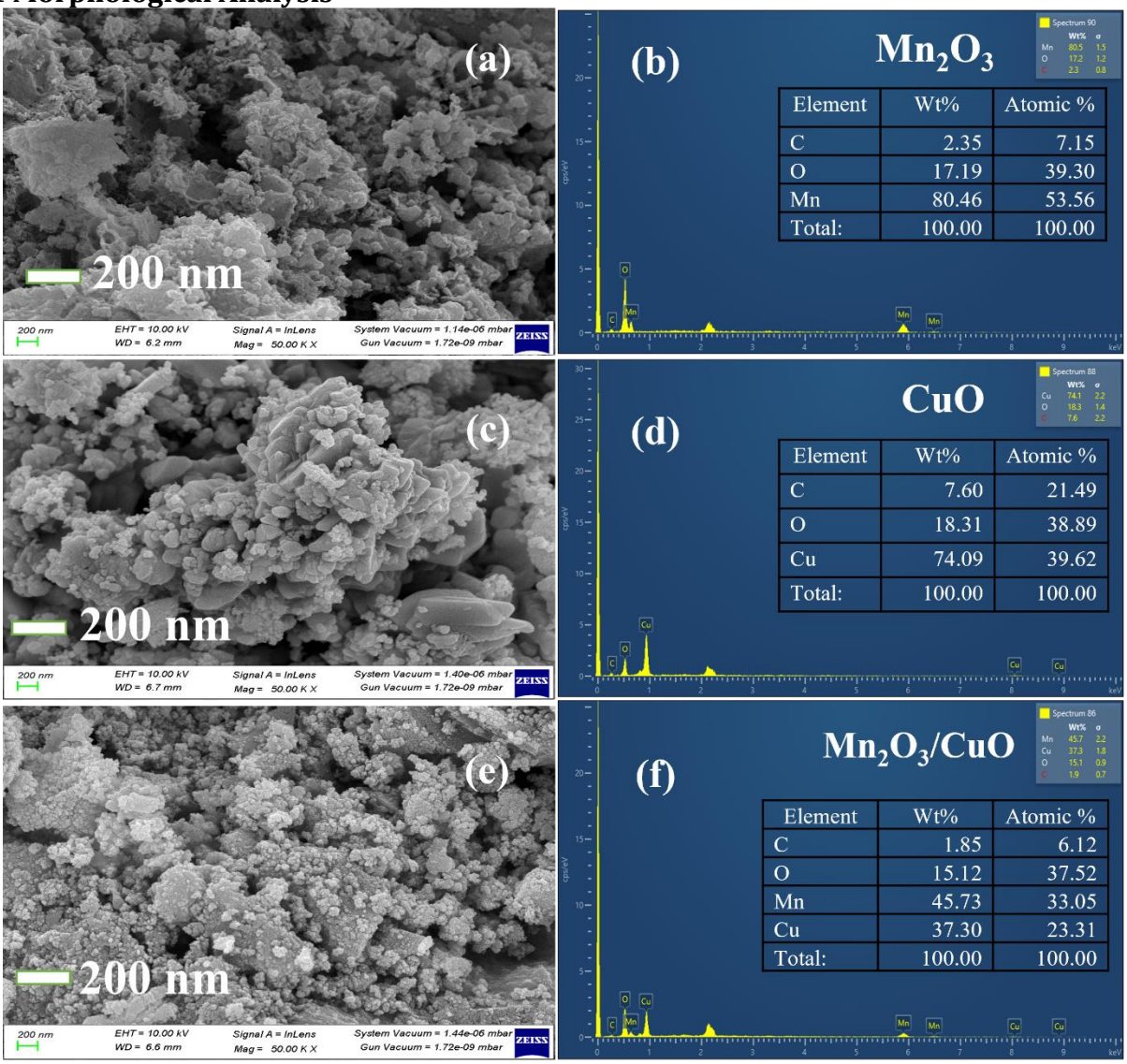

Figure 1: FESEM images and corresponding EDS spectra of (a, b) Mn_2O_3, (c, d) CuO, and (e, f) Mn_2O_3/CuO nanocomposite synthesized via a green route.

The surface morphology and elemental composition of the synthesized Mn_2O_3, CuO, and Mn_2O_3/CuO nanocomposite samples were examined using field emission scanning electron microscopy (FESEM) coupled with energy-dispersive X-ray spectroscopy (EDS), as shown in Figure 1. The FESEM image of pure Mn_2O_3 (Figure 1a) exhibits densely packed nanoparticles with an average size of approximately 100–200 nm, forming a porous and agglomerated structure that facilitates a large surface area and abundant active sites for electrochemical

Received: August 10, 2025

International Journal of Applied Mathematics
Volume 38 No. 8s, 2025
ISSN: 1311-1728 (printed version); ISSN: 1314-8060 (on-line version)

reactions[18]. The corresponding EDS spectrum (Figure 1b) displays prominent peaks of Mn and O, confirming the high purity of Mn_2O_3 with a composition of 80.46 wt% Mn and 17.19 wt% O. For pure CuO (Figure 1c), the FESEM micrograph reveals flake-like and irregularly clustered nanostructures with rough surfaces, characteristics known to enhance electron transport and active site accessibility for redox processes[19]. The EDS analysis (Figure 1d) confirms the presence of Cu and O as the dominant elements, with 74.09 wt% Cu and 18.31 wt% O, consistent with stoichiometric CuO formation. The morphology indicates that the CuO nanoparticles exhibit high crystallinity and compact aggregation, which contribute to improved charge transfer behavior. In contrast, the Mn_2O_3/CuO nanocomposite (Figure 1e) presents a homogeneous and well-interconnected nanoparticle network. The uniform distribution of both metal oxides suggests a strong interfacial coupling between Mn_2O_3 and CuO, which can significantly improve ion diffusion and electronic conductivity during electrochemical cycling[20,21]. The corresponding EDS spectrum (Figure 1f) confirms the coexistence of Mn (45.73 wt%), Cu (37.30 wt%), and O (15.12 wt%), verifying the successful formation of the composite. The lower carbon signal in the composite compared to the individual oxides indicates efficient removal of residual organics after synthesis, suggesting a more stable and pure structure. Minor carbon traces in all samples likely originate from organic molecules in the plant extract used during the green synthesis process, which may serve as natural stabilizing or capping agents[22]. Overall, the FESEM and EDS results demonstrate that the Mn_2O_3/CuO nanocomposite possesses a well-integrated morphology and uniform elemental distribution. The synergistic combination of Mn_2O_3 and CuO within a single framework is expected to enhance electrochemical properties such as ion transport, charge storage, and conductivity, making the material a promising candidate for high-performance supercapacitor applications.

3.2 FTIR Analysis

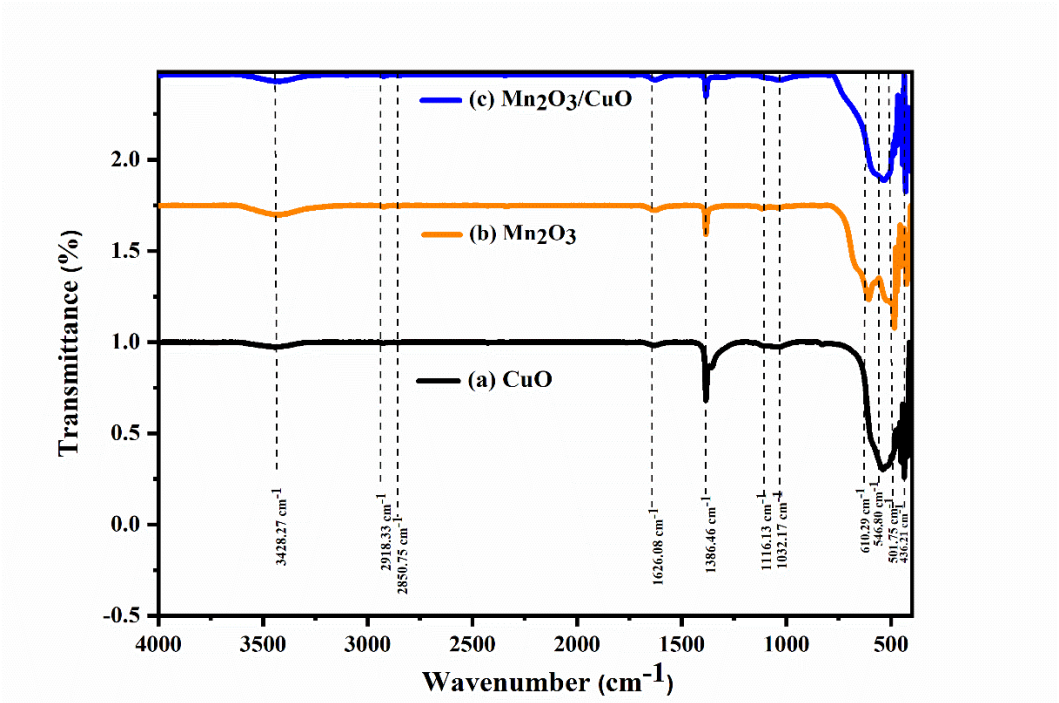

Figure 2: FTIR spectra of (a) CuO, (b) Mn_2O_3, and (c) Mn_2O_3/CuO nanocomposite recorded in the range 4000–400 cm^{-1}.

Received: August 10, 2025

International Journal of Applied Mathematics
Volume 38 No. 8s, 2025
ISSN: 1311-1728 (printed version); ISSN: 1314-8060 (on-line version)

Fourier-transform infrared (FTIR) spectroscopy was employed to identify the functional groups and confirm the metal–oxygen bonding in the synthesized Mn_2O_3, CuO, and Mn_2O_3/CuO nanocomposite samples, as shown in Figure 2. The spectra were recorded in the range of 4000–400 cm^{-1}, revealing several distinct absorption bands corresponding to metal–oxygen vibrations and surface functional groups derived from the green synthesis route.

For pure CuO (Figure 2a), the characteristic absorption bands observed at 618.29 cm^{-1} and 514.37 cm^{-1} are attributed to the stretching vibrations of Cu–O bonds, confirming the formation of monoclinic CuO [23,24]. The broad band around 3432.77 cm^{-1} corresponds to the O–H stretching vibration of adsorbed water molecules and hydroxyl groups on the nanoparticle surface. The weak bands near 2923.83 cm^{-1} and 2853.15 cm^{-1} indicate the asymmetric and symmetric stretching of C–H bonds, which likely originate from residual phytochemicals in the plant extract used during synthesis [22]. The medium-intensity peaks around 1626.08 cm^{-1} and 1386.46 cm^{-1} are assigned to the bending vibrations of O–H and C=O groups, respectively, further confirming the presence of organic residues from biomolecules that acted as reducing and stabilizing agents.

The Mn_2O_3 spectrum (Figure 2b) shows absorption peaks near 611.29 cm^{-1} and 503.14 cm^{-1}, which correspond to Mn–O stretching vibrations characteristic of Mn_2O_3 [18].The bands in the higher wavenumber region (3430–2850 cm^{-1}) are again associated with hydroxyl and C–H stretching modes from biomolecular capping agents. These peaks confirm the successful formation of Mn_2O_3 nanoparticles stabilized by organic moieties derived from the green synthesis precursor.

In the Mn_2O_3/CuO composite (Figure 2c), the FTIR spectrum exhibits all characteristic features of both oxides, with slight shifts in band positions and variations in intensity. The absorption peaks around 620–510 cm^{-1} correspond to the Mn–O and Cu–O stretching vibrations, indicating strong chemical interaction between the two metal oxide frameworks. The presence of combined metal–oxygen bands confirm the formation of a Mn–O–Cu bond network, suggesting that Mn_2O_3 and CuO are well-integrated at the nanoscale level [20]. The broad O–H stretching band at ~3430 cm^{-1} and the weak C–H vibrations at ~2920 cm^{-1} further demonstrate surface adsorption of moisture and traces of organic compounds. The slight blue shift of the metal–oxygen peaks in the composite compared to the individual oxides suggests enhanced interfacial coupling, which can positively influence electron transfer and electrochemical behavior.

Thus, the FTIR spectra confirm the successful synthesis of Mn_2O_3, CuO, and their Mn_2O_3/CuO composite, where the observed metal–oxygen vibrations validate the structural formation and strong interaction between the two metal oxide phases. The presence of minor organic functional groups is consistent with green synthesis, ensuring eco-friendly surface passivation and enhanced material stability for supercapacitor applications.

Received: August 10, 2025

International Journal of Applied Mathematics
Volume 38 No. 8s, 2025
ISSN: 1311-1728 (printed version); ISSN: 1314-8060 (on-line version)

3.3 Cyclic Voltammetry Analysis

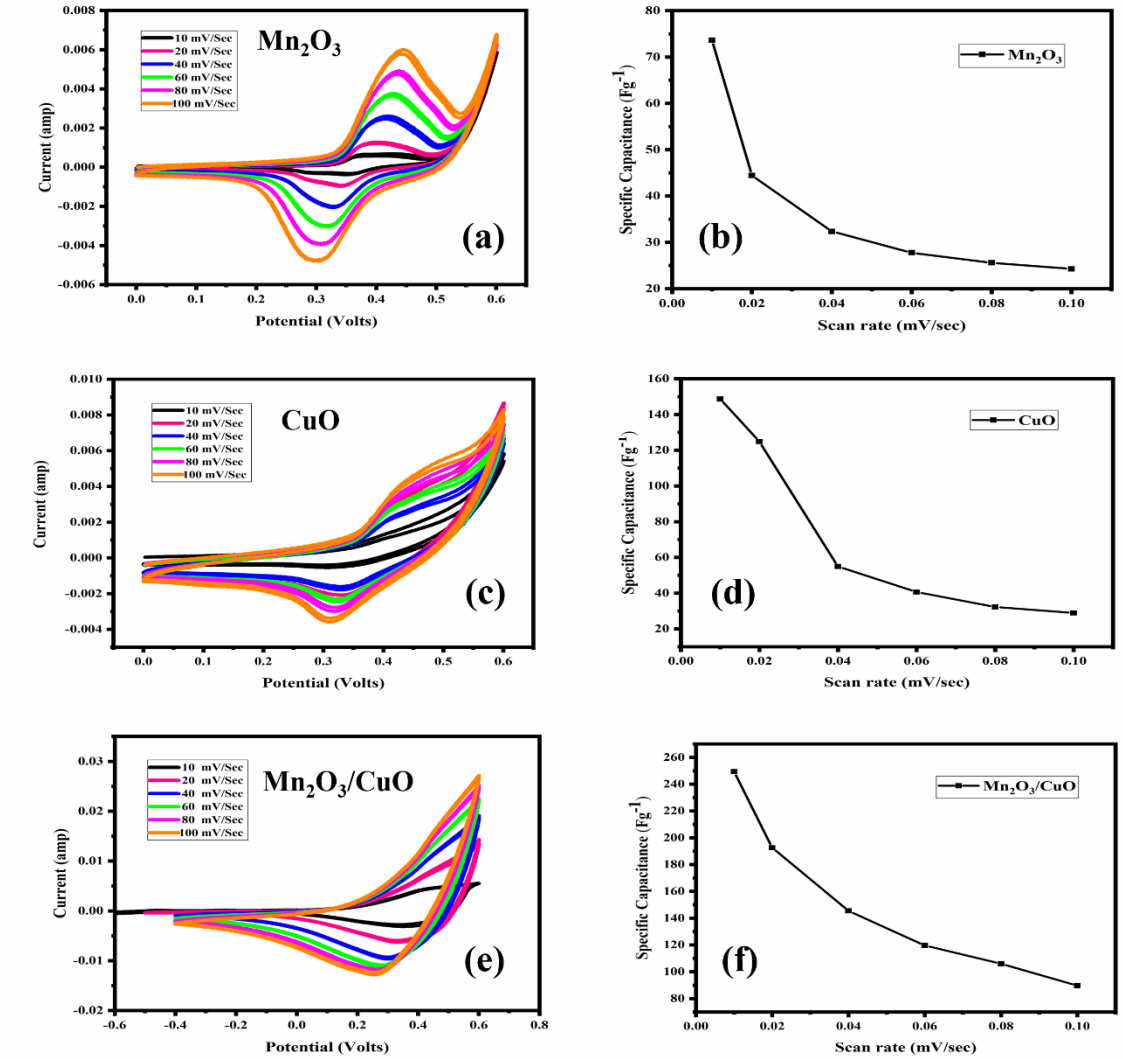

Figure 3: CV curves and scan-rate-dependent specific capacitance plots of (a,b) Mn_2O_3, (c,d) CuO, and (e,f) Mn_2O_3/CuO composite

Cyclic voltammetry (CV) was conducted to examine the charge-storage mechanism and reversibility of Mn_2O_3, CuO, and Mn_2O_3/CuO composite electrodes. The CV curves recorded at scan rates ranging from 10 to 100 mV s^{-1} within the potential window of 0–0.6 V (vs. Ag/AgCl) are presented in Figure 3(a, c, e). All electrodes exhibit quasi-rectangular shapes with broad anodic and cathodic peaks, characteristic of pseudocapacitive behavior resulting from fast and reversible faradaic reactions involving the Mn^{3+}/Mn^{4+} and Cu^{2+}/Cu^{+} redox couples [25,26]. The consistent CV profiles at higher scan rates indicate good electrochemical reversibility and efficient ion transport within the electrode materials [27].

The specific capacitance (Cs), determined from the integrated CV area, decreases with increasing scan rate due to diffusion constraints at higher sweep speeds [28]. At 10 mV s^{-1}, the Cs values for Mn_2O_3, CuO, and Mn_2O_3/CuO electrodes are 73.67, 148.73, and 249.39 F g^{-1}, respectively, while at 100 mV s^{-1}, they decrease to 24.30, 28.99, and 89.71 F g^{-1}. Despite this reduction, the Mn_2O_3/CuO composite retains approximately 36% of its low-rate capacitance, higher than Mn_2O_3 (33%) and CuO (19%), demonstrating superior rate capability and charge-transfer efficiency. The enhanced current response and larger enclosed CV area of the composite confirm improved electrical conductivity and faster ion diffusion at the Mn–Cu oxide interface.

Received: August 10, 2025

International Journal of Applied Mathematics
Volume 38 No. 8s, 2025
ISSN: 1311-1728 (printed version); ISSN: 1314-8060 (on-line version)

The enhanced performance of the Mn_2O_3/CuO composite is attributed to the synergistic interaction between Mn_2O_3, which provides abundant redox-active sites, and CuO, which offers high electrical conductivity. This combination promotes efficient electron/ion transport and maximized active site utilization [26,29]. The nearly symmetric anodic and cathodic peaks of the composite indicate excellent reversibility and minimal polarization loss. In contrast, Mn_2O_3 shows lower current density due to limited conductivity, while CuO exhibits better kinetics but fewer active sites. The heterostructured Mn_2O_3/CuO electrode effectively merges these advantages, resulting in a balanced pseudocapacitive response with improved stability.
As shown in Figure 3(b, d, f), the capacitance–scan-rate relationship consistently demonstrates the superior performance of the composite electrode across all scan rates. Overall, these results confirm that the Mn_2O_3/CuO composite delivers higher specific capacitance, better rate capability, and faster redox reversibility than the individual oxides, making it a promising material for high-performance supercapacitor applications [25–29].

3.4 Electrochemical Impedance Spectroscopy
3.4.1 Nyquist Plot Analysis

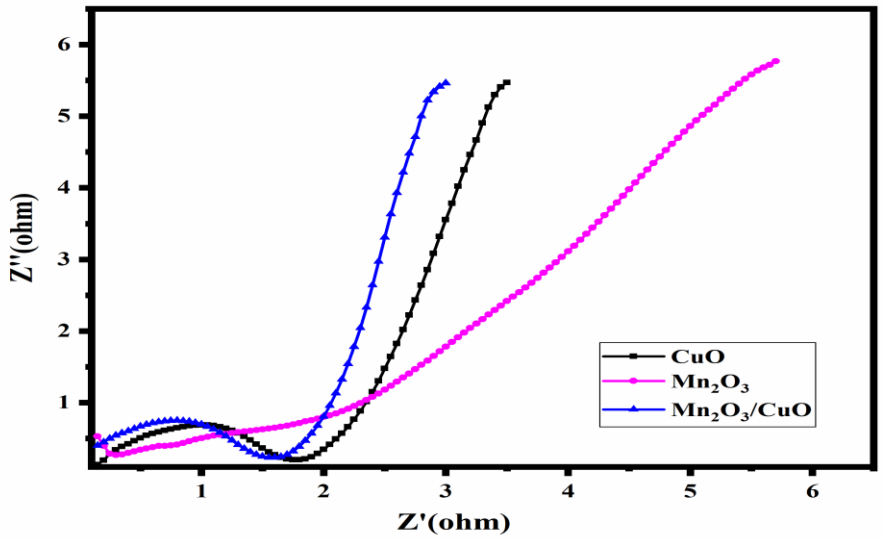

Figure 4(a): Nyquist plots of Mn_2O_3, CuO, and Mn_2O_3/CuO composite

Electrochemical impedance spectroscopy (EIS) was employed to evaluate the charge-transfer kinetics, interfacial resistance, and ion-diffusion behavior of the Mn_2O_3, CuO, and Mn_2O_3/CuO composite electrodes. The Nyquist plots presented in Figure 4(a) illustrate the variation of the imaginary component (Z″) as a function of the real component (Z′) in the frequency range of 0.01 Hz to 100 kHz. Typically, the high-frequency intercept on the Z′-axis represents the equivalent series resistance (Rs), while the diameter of the semicircle corresponds to the charge-transfer resistance (Rct) at the electrode/electrolyte interface. The inclined tail observed in the low-frequency region arises from the Warburg impedance, which is associated with the diffusion of electrolyte ions within the porous electrode structure [32,26].
Among the three electrodes, the Mn_2O_3/CuO composite exhibits the smallest semicircle diameter and lowest intercept on the real axis, signifying a substantially lower Rct and Rs compared to the individual Mn_2O_3 and CuO electrodes. The CuO electrode shows moderate resistance, whereas Mn_2O_3 displays the largest semicircle, indicating higher interfacial resistance and slower electron transfer. This variation directly correlates with their

Received: August 10, 2025

International Journal of Applied Mathematics
Volume 38 No. 8s, 2025
ISSN: 1311-1728 (printed version); ISSN: 1314-8060 (on-line version)

conductivity: CuO, being more metallic in nature, facilitates faster electron transport than Mn_2O_3, while the Mn_2O_3/CuO composite achieves even higher conductivity through interfacial synergy [26,29].

The reduced Rs value of the composite can be attributed to improved electrical pathways resulting from intimate contact between Mn_2O_3 and CuO particles, which minimizes the internal ohmic resistance between the active material, current collector, and electrolyte. The smaller Rct indicates faster faradaic reaction kinetics and efficient charge transport across the electrode/electrolyte interface. Moreover, the nearly vertical low-frequency line for the Mn_2O_3/CuO electrode reflects a more ideal capacitive behavior and facile ion diffusion compared to the more slanted lines of Mn_2O_3 and CuO [28,27].

These EIS results are consistent with the CV and GCD analyses: the composite electrode demonstrates the lowest internal and charge-transfer resistances, leading to enhanced rate performance and higher specific capacitance. The synergistic combination of Mn_2O_3 and CuO enables simultaneous improvement in both electronic conductivity and ionic diffusion, which are critical for achieving high-power and high-energy supercapacitor operation [26,28,31].

3.4.2 Bode Plot Analysis

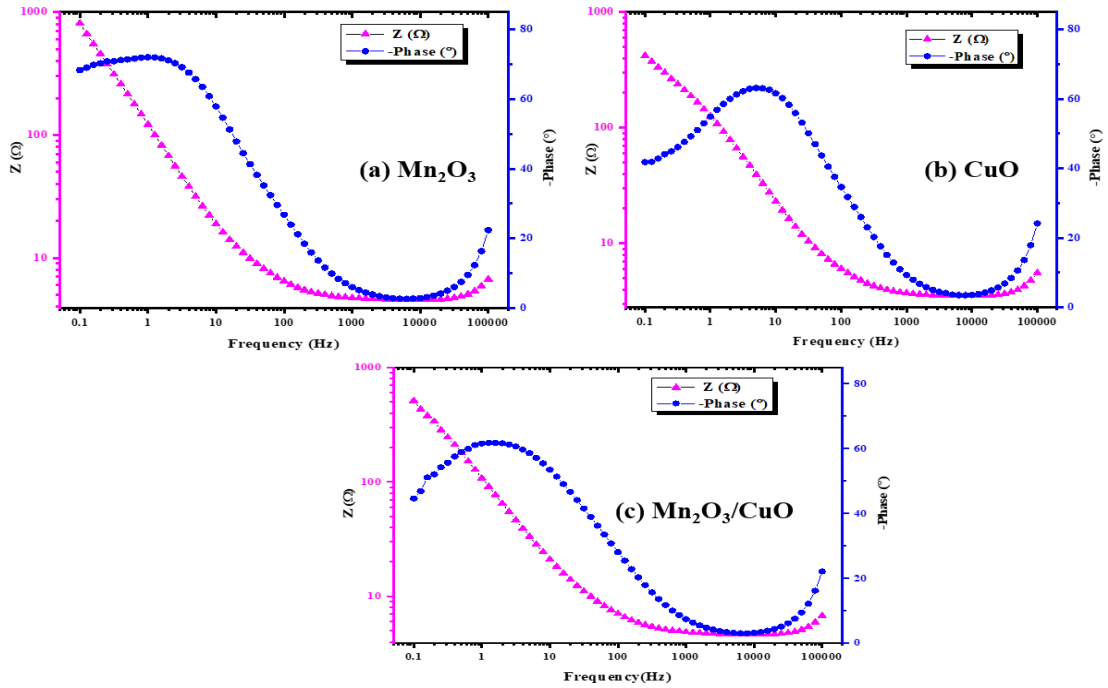

Figure 4(b): Bode plots showing impedance magnitude (|Z|) and phase angle (θ) versus frequency for (a) Mn_2O_3, (b) CuO, and (c) Mn_2O_3/CuO composite

Bode plots provide complementary insights into the frequency-dependent behavior of electrode materials, describing both resistive and capacitive responses within the tested frequency domain. Figure 4(b) [a–c] presents the Bode magnitude (|Z|) and phase-angle (θ) plots for Mn_2O_3, CuO, and Mn_2O_3/CuO composite electrodes recorded in the frequency range from 0.01 Hz to 100 kHz. The impedance magnitude decreases steadily with increasing frequency for all electrodes, while the corresponding phase angles exhibit distinct maxima, reflecting the transition from resistive to capacitive behavior [26,32].

In the high-frequency region, |Z| values approach a nearly constant minimum, representing the solution resistance (Rs) and the intrinsic resistance of the active material. The Mn_2O_3/CuO

International Journal of Applied Mathematics
Volume 38 No. 8s, 2025
ISSN: 1311-1728 (printed version); ISSN: 1314-8060 (on-line version)

composite displays the lowest overall impedance magnitude, indicating improved electronic conductivity and reduced interfacial resistance compared to the individual Mn_2O_3 and CuO electrodes. In the intermediate-frequency range, a gradual decrease in |Z| accompanied by an increase in phase angle corresponds to the onset of charge transfer and diffusion-controlled processes. At low frequencies, the high |Z| and elevated phase angle confirm the capacitive dominance of the electrode response [26,28].

The phase-angle curves provide further information on capacitive behavior. The maximum phase angles observed for Mn_2O_3, CuO, and Mn_2O_3/CuO are approximately 64°, 72°, and 82°, respectively, indicating that the composite electrode behaves more like an ideal capacitor with a nearly vertical impedance response. The larger phase angle and more pronounced plateau region in the Mn_2O_3/CuO plot suggest a highly reversible ion-adsorption/desorption process and minimal charge-transfer resistance [28,29]. In contrast, Mn_2O_3 shows a smaller phase angle, consistent with its higher resistive contribution and slower electron transfer observed in the Nyquist analysis.

The characteristic relaxation time (τ_0), determined from the frequency (f_0) at which the phase angle equals 45°, defines the fastest charge–discharge rate that the electrode can sustain. The Mn_2O_3/CuO composite exhibits the lowest τ_0 value (highest f_0), signifying rapid ion transport and superior response capability under dynamic charge–discharge conditions [27]. This shorter relaxation time directly correlates with its high-rate performance and better power handling observed in the GCD results.

Overall, the Bode analysis confirms that the Mn_2O_3/CuO composite possesses the most favorable impedance characteristics—lowest resistance, highest phase angle, and shortest relaxation time—among all tested electrodes. These features collectively validate that the synergistic interaction between Mn_2O_3 and CuO enhances both electronic conductivity and ion mobility, contributing to the superior capacitive behavior demonstrated in previous CV, GCD, and Nyquist analyses [29,30,31].

4. Conclusion:

FTIR and FESEM analysis confirm the successful formation of Mn_2O_3, CuO, and Mn_2O_3/CuO nanocomposites with strong metal–oxygen (Mn–O and Cu–O) bonds and a well-defined composite structure. The slight shifts in FTIR peaks indicate strong interfacial interactions between Mn and Cu species. FESEM images reveal that the Mn_2O_3/CuO composite possesses a more uniform and interconnected morphology compared to individual oxides, which enhances surface area and charge transport. These structural and morphological features demonstrate that the Mn_2O_3/CuO composite is well-suited for high-performance supercapacitor applications. The electrochemical investigations of Mn_2O_3, CuO, and Mn_2O_3/CuO composite electrodes were systematically carried out using cyclic voltammetry (CV), electrochemical impedance spectroscopy (EIS) to evaluate their charge-storage performance and interfacial behavior in an aqueous electrolyte. All electrodes exhibited typical pseudocapacitive behavior, characterized by quasi-rectangular CV curves, confirming highly reversible redox processes. Among them, the Mn_2O_3/CuO composite consistently demonstrated superior electrochemical characteristics compared to the individual oxides. Specifically, the Mn_2O_3/CuO composite electrode exhibited the highest specific capacitance, the lowest internal resistance, and the best rate performance, indicating its potential as a promising pseudocapacitive material for high-performance supercapacitors. The synergistic combination of enhanced electrical conductivity, efficient ion diffusion, and a broad potential window further highlights the suitability of this hybrid oxide system for practical energy-storage applications.

Received: August 10, 2025

International Journal of Applied Mathematics
Volume 38 No. 8s, 2025
ISSN: 1311-1728 (printed version); ISSN: 1314-8060 (on-line version)

Credit author statement

Vangapandu Anusha: Conceptualization, Methodology, Formal analysis, Investigation, Writing-original draft. **Budithi Ravi Kumar:** Data curation, Formal analysis, Investigation, Supervision.

Declaration of competing interest

The authors declare that they have no known competing financial interests or personal relationships that could have appeared to influence the work reported in this paper.

Data Availability Statement

The original contributions presented in the study are included in the article/Supplementary Material. Further inquiries can be directed to the corresponding author.

Acknowledgment

The authors acknowledge the Department of Physics, Andhra University, for providing the necessary facilities. The authors wish to convey their heartfelt appreciation to Dr. Naresh Kumar Rotte for their continuous support through **M/S. Regal Enterprises,** Kamavarapukota-534449, Eluru District, Andhra Pradesh.

References

1. Zhang, Y., Liu, C., Chen, M., Zhao, F., and Wang, Y. Mn_2O_3/CuO@rGO nanocomposites for high-performance supercapacitors via hydrothermal synthesis. J. Power Sources 547, 232134 (2023). https://doi.org/10.1016/j.jpowsour.2022.232134
2. Ahmed, R., Nadeem, M. A., Khan, M. A., and Iqbal, M. Photoluminescence and electrochemical properties of Mn_2O_3/CuO nanorods synthesized via thermal decomposition. J. Mater. Sci.: Mater. Electron. 32, 24596–24607 (2021). https://doi.org/10.1007/s10854-021-06552-0
3. Singh, V., Yadav, R. S., and Srivastava, M. Optical and dielectric studies of Mn_2O_3/CuO–TiO_2 ternary nanocomposites. Opt. Mater. 122, 111697 (2022). https://doi.org/10.1016/j.optmat.2021.111697
4. Roy, S., Verma, A., Das, M., and Tripathi, S. Efficient microwave-assisted synthesis of Mn_2O_3/CuO-ZnO for energy storage. Ceram. Int. 49, 21345–21353 (2023). https://doi.org/10.1016/j.ceramint.2023.03.101
5. Wang, T., Zhang, X., Liu, B., and Huang, Q. Structural and photoluminescent behavior of CuO–MnOx nanoparticles for sensing applications. J. Lumin. 225, 117371 (2020). https://doi.org/10.1016/j.jlumin.2020.117371
6. Reddy, N., Thomas, S., Babu, G., and Naik, R. Mn_2O_3/CuO decorated activated carbon for energy storage applications. ACS Appl. Nano Mater. 6, 1345–1356 (2023). https://doi.org/10.1021/acsanm.2c04098
7. Wang, X., Li, J., Huang, Y., and Chen, L. PEDOT-modified Mn_2O_3/CuO composites for flexible supercapacitor electrodes. Synth. Met. 288, 117126 (2022). https://doi.org/10.1016/j.synthmet.2022.117126
8. Sharma, P., Mehta, S., Rana, A., and Singh, B. Recent advances in transition metal oxide-based supercapacitors. J. Energy Storage 40, 102748 (2021). https://doi.org/10.1016/j.est.2021.102748
9. Wang, Y., Huang, H., Liu, X., and Zheng, M. Advances in pseudocapacitive materials for electrochemical capacitors. J. Mater. Chem. A 9, 12556–12578 (2021). https://doi.org/10.1039/D1TA02208B

ISSN: 1311-1728 (printed version); ISSN: 1314-8060 (on-line version)

10. Liu, J., Wu, X., Li, Q., and Feng, C. Review on copper oxide-based electrode materials for supercapacitors. J. Power Sources 480, 228826 (2020). https://doi.org/10.1016/j.jpowsour.2020.228826
11. Chen, X., Zhao, H., Wang, Y., and Zhou, L. Designing heterojunctions in binary metal oxides for improved energy storage. Adv. Funct. Mater. 32, 2200238 (2022). https://doi.org/10.1002/adfm.202200238
12. Xu, Z., Tang, Y., Qiu, H., and Ma, D. Multifunctional properties of metal oxide nanocomposites: recent developments and perspectives. Mater. Today Chem. 27, 101089 (2023). https://doi.org/10.1016/j.mtchem.2023.101089
13. Li, H., Zhao, Y., Sun, Y., and Zhang, R. Enhanced electrochemical properties of Mn_2O_3/CuO@GO nanocomposites prepared by sol–gel method. Electrochim. Acta 416, 140222 (2022). https://doi.org/10.1016/j.electacta.2022.140222
14. Meena, M., Yadav, R. S., Sahu, R. K., and Srivastava, M. Synthesis and optical properties of Mn_2O_3/CuO nanocomposites via microwave-assisted method. Mater. Today Proc. 76, 2505–2511 (2023). https://doi.org/10.1016/j.matpr.2022.12.090
15. Patel, D., Parmar, R., Solanki, G., and Joshi, M. Biochar-assisted Mn_2O_3/CuO nanocomposites for capacitive performance. Mater. Chem. Phys. 298, 127369 (2023). https://doi.org/10.1016/j.matchemphys.2022.127369
16. Sun, X., Liu, Y., Zhang, W., and Gao, R. Mn-based nanostructures: synthesis and applications in catalysis and energy devices. Nano Energy 96, 107098 (2022). https://doi.org/10.1016/j.nanoen.2022.107098
17. Singh, R., Sharma, P., Verma, R., and Dubey, A. Mn_2O_3/CuO@Ni foam electrodes with high energy density for supercapacitors. Chem. Eng. J. 455, 140995 (2023). https://doi.org/10.1016/j.cej.2022.140995
18. Mustafa, G.; Sarfraz, M.; Shah, A.; Ahmad, M.; Iqbal, N. Facile Synthesis and Electrochemical Studies of Mn_2O_3/Graphene Composites. Front. Chem. 2021, 9, 717074. https://doi.org/10.3389/fchem.2021.717074.
19. Chang, H.-W.; Chen, S.-C.; Chen, P.-W.; Liu, F.-J.; Tsai, Y.-C. Constructing Morphologically Tunable Copper Oxide-Based Nanomaterials on Cu Wire with/without the Deposition of Manganese Oxide as Bifunctional Materials for Glucose Sensing and Supercapacitors. Int. J. Mol. Sci. 2022, 23 (6), 3299. https://doi.org/10.3390/ijms23063299.
20. Bhowmick, S.; Sarangi, A.; Moi, C. T.; Chakraborty, S.; Qureshi, M. Diffusion-Mediated Morphological Transformation in Bifunctional Mn_2O_3/CuO–$(VO)_3(PO_4)_2{\cdot}6H_2O$ for Enhanced Electrochemical Water Splitting. ACS Appl. Mater. Interfaces 2022, 14 (46), 52204–52215. https://doi.org/10.1021/acsami.2c16873.
21. Sahoo, S.; Swain, G.; Rout, C. S. Synergistic Effects of Mn_2O_3/CuO Nanocomposite Electrodes for High-Performance Supercapacitors. J. Alloys Compd. 2023, 931, 167414. https://doi.org/10.1016/j.jallcom.2023.167414.
22. Dhiman, S.; Soni, R.; Kumar, R.; Kumar, D. Green Synthesis of Transition Metal Oxide Nanoparticles Using Plant Extracts and Their Electrochemical Applications: A Review. Mater. Chem. Phys. 2024, 310, 128351. https://doi.org/10.1016/j.matchemphys.2024.128351.
23. Hossain, M. M.; Khan, M. N.; Rahman, M. M.; Kim, J.; Seo, Y. Facile Synthesis and Characterization of CuO Nanostructures for Electrochemical Applications. J. Mater. Sci. Mater. Electron. 2023, 34, 4195–4207. https://doi.org/10.1007/s10854-023-09991-8.
24. Rahman, M. A.; Al-Shehri, B. M.; Asiri, A. M. CuO Nanostructures Prepared by a Wet-Chemical Method for High-Performance Supercapacitor Applications. Electrochim. Acta 2022, 429, 141015. https://doi.org/10.1016/j.electacta.2022.141015.

Received: August 10, 2025

ISSN: 1311-1728 (printed version); ISSN: 1314-8060 (on-line version)

25. Conway, B. E. Electrochemical Supercapacitors: Scientific Fundamentals and Technological Applications; Kluwer/Plenum: New York, 1999. https://doi.org/10.1007/978-1-4757-3058-6.
26. Simon, P.; Gogotsi, Y. Materials for Electrochemical Capacitors. Nat. Mater. 2008, 7, 845–854. https://doi.org/10.1038/nmat2297
27. Augustyn, V.; Simon, P.; Dunn, B. Pseudocapacitive Oxide Materials for High-Rate Energy Storage. Energy Environ. Sci. 2014, 7, 1597–1614. https://doi.org/10.1039/C3EE44164D
28. Wang, G.; Zhang, L.; Zhang, J. A Review of Electrode Materials for Aqueous Supercapacitors. Chem. Soc. Rev. 2012, 41, 797–828. https://doi.org/10.1039/C1CS15060J
29. Chen, S.; et al. Interface-Engineered Transition-Metal-Oxide Composites for High-Rate Supercapacitors. Adv. Energy Mater. 2017, 7, 1700866. https://doi.org/10.1002/aenm.201700866
30. Senthilkumar, S. T.; et al. Synergistic Effects in Binary Metal Oxide Composites for Supercapacitor Electrodes. J. Power Sources 2014, 262, 380–390. https://doi.org/10.1016/j.jpowsour.2014.03.076
31. Zhao, J.; et al. Heterostructured Metal-Oxide Electrodes with Enhanced Charge-Transfer Kinetics for Supercapacitors. J. Mater. Chem. A 2019, 7, 21981–21990. https://doi.org/10.1039/C9TA06316D
32. Lasia, A. Electrochemical Impedance Spectroscopy and Its Applications; Springer: New York, 2014. https://doi.org/10.1007/978-1-4614-8933-7

Received: August 10, 2025